JBP
Journal of Biochemicals and Phytomedicine
eISSN: 2958-8561

Biochemical and Antimicrobial Studies of Metallic Nanoparticles Synthesized from *Justicia carnea* Extract: Molecular Docking of Its Phytochemicals for Anti-Anaemic Potential

Adebayo Seun Gbadamosi [1*], Oloketuyi Kikelomo Boluwatife [2], Margaret Oladunni Oseni [3], Olatunde Abass Oseni [4]

[1] National Biotechnology Research and Development Agency, Abuja, Nigeria
[2] Department of Science Laboratory Technology, Ekiti State University, Ado-Ekiti, Nigeria
[3] Department of Chemistry, Federal University, Oye-Ekiti, Nigeria
[4] Department of Medical Biochemistry, College of Medicine, Ekiti State University, Ado-Ekiti, Nigeria

ARTICLE INFO

Article Type:
Research

Article History:
Received: 29 May 2025
Revised: 18 Aug 2025
Accepted: 10 Sept 2025
Available online: 8 Jan 2026

Keywords:
Natural products,
Molecular docking,
Anaemia,
Nanoparticles,
Antimicrobial activities,
Justicia carnea

** Corresponding author:*
E-mail:
adebayoseungbadamosi@gmail.com

ABSTRACT

Introduction: Anaemia affects over 1.6 billion people worldwide. This study explored *Justicia carnea* and its green-synthesized metallic nanoparticles as potential anti-anaemic agents, combining biochemical evaluation and molecular docking of key phytochemicals
Methods: Phytochemical composition, antioxidant capacity, antimicrobial activity, and green synthesis of three metallic NPs were analyzed using standard techniques. Eight phytochemicals were docked against anaemia-related targets (EPOR, MIF, ERα, transferrin, DHFR) using SwissDock. Binding interactions were profiled with PLIP, and drug-likeness predicted with SwissADME.
Results: Screening revealed bioactive constituents including steroids, alkaloids, flavonoids, phenols, and terpenoids, indicating broad medicinal potential. The extract showed strong antioxidant activity and free-radical scavenging, potentially mitigating oxidative stress associated with anaemia. Significant antifungal activity was observed in the extract, whereas the NPs exhibited notable antibacterial effects. FTIR confirmed phenolics, carboxylic acids, and amines. Docking revealed ursolic acid binding EPOR ($\Delta G = -7.82$ kcal/mol), rosmarinic acid interacting with ERα, β-amyrin and ursolic acid targeting MIF, and rutin binding transferrin ($\Delta G = -8.69$ kcal/mol), supporting iron transport. Kaempferol and rosmarinic acid displayed favorable ADME profiles, suggesting drug-like potential.
Conclusion: *J. carnea* and its biosynthesized nanoparticles demonstrate significant antioxidant, antimicrobial, and anti-anaemic activities, highlighting their potential as safe, cost-effective, and multifunctional therapeutic agents against anaemia.

Please cite this paper as:
Gbadamosi AS, Oloketuyi KB, Oseni MO, Oseni OA. Biochemical and antimicrobial studies of metallic nanoparticles synthesized from *Justicia carnea* extract: molecular docking of its phytochemicals for anti-anaemic potential. Journal of Biochemicals and Phytomedicine. 2026; 5(1): 1-15. doi: 10.34172/jbp.2026.1.

Introduction

Despite progress in global healthcare, anemia continues to pose a major public health challenge, especially across low- and middle-income nations (McLean et al., 2011). The World Health Organization identifies it as one of the leading yet preventable causes of mortality among young children and pregnant women living in malaria-endemic areas (WHO, 2023). Anemia is marked by a reduced red blood cell count or quality, which impairs oxygen delivery throughout the body. It occurs in several forms, including iron-deficiency, megaloblastic, and hemolytic anemia each with distinct causes and clinical implications. Among these, iron-deficiency anemia is the most prevalent, accounting for nearly 50% of global cases and often arising from inadequate dietary iron, blood loss, or malabsorption (Kassebaum et al., 2014). Clinical symptoms range from fatigue, pallor, and shortness of breath to cognitive impairment and reduced productivity.

Although synthetic iron supplements are widely used, their high cost, poor tolerability, and limited accessibility, especially in resource-limited settings, hinder treatment compliance. These limitations have driven interest in alternative approaches such as nanoparticle-based iron formulations, which have demonstrated enhanced absorption and reduced gastrointestinal side effects (Kumar and Kumbhat, 2016). In parallel, plant-based therapies have gained attention for their affordability, accessibility, and cultural acceptance. A variety of secondary metabolites including flavonoids, alkaloids, and saponins account for the pharmacological potential of many medicinal plants, conferring antioxidant, antimicrobial, and anti-inflammatory benefits (Atanasov et al., 2021). These attributes make them valuable candidates for managing anemia and its related complications through natural therapeutic pathways.

Justicia carnea, commonly known as "blood of Jesus" in Nigeria, is a medicinal plant from the Acanthaceae family. Though native to South America, it is widely cultivated in tropical Africa for both ornamental and therapeutic purposes (Anarado et al., 2021; Igbinaduwa et al., 2020). The plant is characterized by vibrant pink flowers, broad green leaves, and a high level of adaptability to diverse climatic conditions. Traditionally, it is used to treat conditions such as anemia, inflammation, sickle cell disease, and malaria (Badami et al., 2003; Onyeabo et al., 2017). Phytochemical studies have identified flavonoids, alkaloids, phenolics, terpenoids, and saponins in the plant, which may contribute to its therapeutic effects by modulating biochemical pathways, enhancing immune responses, and promoting tissue repair. Plant-based iron supplements derived from *J. carnea* have also demonstrated higher bioavailability than synthetic counterparts (Zhao et al., 2022), and the plant's influence on haematopoiesis has been shown to improve red blood cell production and haemoglobin levels in anemic models.

The application of nanotechnology in phytochemistry has opened new avenues for enhancing therapeutic efficacy. By integrating nanotechnology with phytochemicals, synergistic effects can be achieved, boosting biological activity particularly in disease models involving oxidative stress, microbial infections, and cancer. Metallic nanoparticles such as copper (CuNPs), zinc oxide (ZnO NPs), gold (AuNPs), and silver (AgNPs), possess notable biofunctional properties, making them suitable for addressing microbial resistance and enhancing pharmacokinetic performance. In anemia therapy, nano-iron formulations have been shown to improve intestinal absorption and reduce gastrointestinal discomfort relative to standard oral iron therapies (Kumar and Kumbhat, 2016).

Molecular docking is a computational strategy that predicts how small molecules interact with specific protein sites and have become integral to modern drug-discovery pipelines. It allows researchers to virtually screen phytochemicals for their affinity and selectivity toward enzymes or receptors linked to disease processes (Meng et al., 2022). In studies of anemia, this approach helps reveal possible bindings between plant-derived molecules and proteins regulating erythropoiesis or iron metabolism. This study combines traditional medicinal knowledge with nanotechnology and computational biology to explore novel, plant-based strategies for the effective and accessible treatment of anemia.

Materials and Methods

Collection, Processing, and Extraction of Plant Material

Fresh *J. carnea* leaves were obtained from Ikorodu, Lagos State, Nigeria, on September 19, 2024. The collected samples were initially washed with clean tap water and subsequently rinsed with distilled water to eliminate adhering dust and impurities. The leaves were then allowed to air-dry under ambient laboratory conditions until completely moisture-free before being ground into a fine powder using an electric blender. Approximately 52.92 g of the pulverized sample was macerated in 500 mL of distilled water within a 1 L round-bottom flask and subjected to heating for one hour using a controlled heating mantle. The resulting mixture was successively filtered first through standard filter paper and then through cotton wool to yield a clear aqueous extract. The filtrate was preserved in airtight containers and refrigerated at 4 °C pending subsequent analyses.

Phytochemical Screening

The aqueous extract of *J. carnea* leaves was screened qualitatively for secondary metabolites such as phlobatannins and phenols using standard phytochemical assays in accordance with Harborne (1973) and Trease and Evans (1996).

Antioxidant Assays

Antioxidant activities of the extract were determined using established standard procedures as follows:

The DPPH radical scavenging assay was performed according to a modified procedure described by Brand-Williams et al. (1995), and absorbance was measured at 517 nm.

Nitric oxide (NO) radical scavenging activity was assessed using a modified procedure based on Green et al. (1982), with absorbance measured at 546 nm.

Ferric reducing antioxidant power (FRAP) was determined following the modified method of Benzie and Strain (1996), and absorbance was measured at 593 nm.

Lipid peroxidation inhibition (TBARS assay) was performed using the modified method of Ohkawa et al. (1979), and absorbance was measured at 532 nm.

Fe^{2+} chelating ability was evaluated according to the modified method of Dinis et al. (1994), and absorbance was measured at 562 nm.

Total phenolic content was determined by the method of Singleton et al. (1999) using gallic acid as a standard, and absorbance was measured at 765 nm.

Total flavonoid content was analyzed using the modified method of Zhishen et al. (1999), and absorbance was measured at 510 nm.

Vitamin C content was determined by the DNPH method of Roe and Kuether (1943) using bromine water oxidation, and absorbance was measured at 520 nm.

Green Synthesis of Metallic Nanoparticles

The stored *J. carnea* aqueous extract served as the reducing and stabilizing agent for nanoparticle synthesis.

The green synthesis of silver, zinc, and copper nanoparticles was carried out according to the procedures reported by Salem et al. (2023) and Rana et al. (2023), with minor modifications. Equal volumes of 0.1 M metal salt solutions and *J. carnea* aqueous extract were mixed under continuous stirring until a visible color change confirmed nanoparticle formation.

Characterization of Nanoparticles

The formation of silver (AgNPs), zinc (ZnNPs), and copper (CuNPs) nanoparticles was confirmed spectroscopically using ultraviolet–visible (UV–Vis) analysis. The optical characteristics of the reaction mixtures were monitored with a double-beam spectrophotometer (Shimadzu UV-1800, Kyoto, Japan) across the wavelength range of 300–800 nm, with a spectral resolution of 1 nm, following the method outlined by Altınsoy et al. (2024). Distilled water served as the reference solution for all measurements. Fourier-transform infrared spectroscopy (FTIR) was subsequently employed to identify the organic functional groups present in both the *J. carnea* aqueous extract and the synthesized nanoparticles. The FTIR spectra were obtained according to the approach reported by Singh et al. (2023).

Antimicrobial Analysis

The antibacterial and antifungal potentials of both the *J. carnea* extract and the biosynthesized nanoparticles were examined. Each sample (50 mg) was dissolved in 2 mL of distilled water and mildly heated to achieve complete solubilization. The prepared solutions were transferred into sterile Petri plates, where antimicrobial discs were placed to allow pre-diffusion into the respective samples. The antimicrobial efficacy was determined using the disc diffusion technique as outlined by Gowda et al. (2023), with minor procedural modifications to suit experimental conditions.

Molecular Docking

Ligand Preparation

Eight phytochemicals from J. carnea were modeled using canonical SMILES obtained from PubChem (Kim et al., 2023). Structures were converted and minimized using Open Babel.

Protein Target Retrieval and Preparation

Five anemia-related protein structures, including transferrin and the erythropoietin receptor, were sourced from the Protein Data Bank (Berman et al., 2000). The protein structures were cleaned using PyMOL (Schrödinger, 2015) and prepared for docking using Auto Dock Tools (Morris et al., 2009).

Docking Simulations

Docking analyses were carried out using SwissDock (Gfeller et al., 2014). Binding energies and inhibition constants were recorded, and the best binding poses were selected for further analysis.

Protein–Ligand Interaction Analysis

PLIP (Salentin et al., 2015) was used to analyze hydrogen bonding, hydrophobic interactions, and π–π stacking. All protein–ligand complexes were visualized and rendered in PyMOL (Schrödinger, 2015).

ADME and Drug-Likeness Prediction

Pharmacokinetic properties, including gastrointestinal absorption, blood–brain barrier Gpermeability, CYP450 inhibition, and compliance with Lipinski's rule compliance, were predicted using SwissADME (Daina et al., 2017).

Results

J. carnea contains several secondary metabolites, with terpenoids and steroids highly abundant, while saponins, phenols, flavonoids, alkaloids, and phlobatannins were moderately present. Cardiac glycosides were absent.

As presented in table 1, *J. carnea* exhibited moderate to strong antioxidant potential based on both its phytochemical composition and free radical scavenging performance. Among the activity assays, lipid peroxidation inhibition (42.81 ± 2.64%) and nitric oxide scavenging (41.68 ± 2.64%) showed the highest activities, followed by DPPH radical scavenging (36.07 ± 0.57%), while ferric reducing antioxidant power (FRAP) and Fe^{2+} chelation recorded comparatively lower values. The antioxidant composition further supports these observations, as the extract contained appreciable levels of vitamin C (24.20 ± 0.01 mg/g), total phenolic compounds (19.73 ± 0.10 mg/g), and flavonoids (5.81 ± 0.01 mg/g). The combined presence of these bioactive constituents and the observed functional antioxidant activities confirm the strong free radical scavenging capacity of *J. carnea*.

J. carnea and its metal nanoparticles exhibited varying antibacterial effects across all tested organisms (Table 2). The extract showed mild inhibition, whereas ZnNPs and AgNPs displayed greater activity. ZnNPs showed strong effects against Xanthomonas azonopodis (8 mm) and Pseudomonas aeruginosa (14 mm), while AgNPs were most effective against P. aeruginosa (14 mm) and Streptococcus mutans (8 mm). The streptomycin standard produced the widest inhibition zones.

As shown in table 3, *J. carnea* and its nanoparticles exhibited moderate antifungal effects compared to the standard ketoconazole. The crude extract showed the highest inhibition against Aspergillus flavus (50.78%) and Fusarium oxysporium (47.62%), while CuNPs displayed moderate activity against A. flavus (43.82%). The standard produced near-complete inhibition across all fungi.

As presented in table 4, all ligands exhibited favorable binding affinities ($\Delta G < 0$ kcal/mol) with the selected anti-anaemic target proteins, indicating spontaneous interactions. Rutin showed the strongest overall binding, particularly with transferrin (–8.69 kcal/mol) and macrophage migration inhibitory factor (–8.32 kcal/mol), followed by β-amyrin (–8.90 kcal/mol) and ursolic acid (–8.06 kcal/mol) against MIF.

As shown in table 5, the predicted inhibition constants derived from the docking free energies reveal strong target affinities in the micromolar range. Rutin displayed the lowest Ki values for transferrin (0.42 μM) and MIF (0.80 μM), followed by β-amyrin (0.30 μM) and ursolic acid (1.23 μM) against MIF and EPO, respectively. These low Ki values corroborate their high binding affinities, suggesting potent and stable ligand–receptor interactions relevant to anti-anaemic activity.

The best-binding ligand for each target determined by the lowest ΔG and corresponding Ki, is summarized in table 6—highlighting Rutin for transferrin and ERα, β-amyrin for MIF and DHFR, and ursolic acid for EPO.

As shown in table 7, most *J. carnea* phytoconstituents demonstrated favorable pharmacokinetic profiles with high gastrointestinal (GI) absorption and good bioavailability scores. Quercetin, kaempferol, phytol, and rosmarinic acid showed high GI absorption and acceptable solubility, while rutin, β-amyrin, α-amyrin, and ursolic acid exhibited low absorption and poor solubility. Phytol was the only compound predicted to cross the blood–brain barrier (BBB), and all compounds showed minimal violations of Lipinski's rule, supporting their potential oral bioavailability.

As shown in table 8, PLIP interaction profiling revealed that the lead phytochemicals formed stable complexes with their respective protein targets through hydrogen bonding and hydrophobic interactions. β-Amyrin and ursolic acid both interacted strongly with MIF via key residues such as Asn98, Leu59, and His, suggesting anti-inflammatory potential relevant to anaemia of chronic disease. Rutin exhibited multiple hydrogen bonds with transferrin (Asp63, Lys206), indicating strong affinity for iron-binding regulation, while rosmarinic acid engaged ERα through Glu353 and His residues, implying a modulatory effect on erythropoietic signaling.

Table 1: Antioxidant composition and free radical scavenging activities of *Justicia carnea* extract

Category	Parameter	Value (Mean ± SD)	Unit
Antioxidant Composition	Flavonoids	5.81 ± 0.01	mg/g
	Vitamin C (ascorbic acid)	24.20 ± 0.01	mg/g
	Total phenolic compounds	19.73 ± 0.10	mg/g
Free Radical Scavenging Activity	DPPH radical scavenging activity	36.07 ± 0.57	%
	Lipid peroxidation inhibition	42.81 ± 2.64	%
	Ferric reducing antioxidant power (FRAP)	16.66 ± 0.40	%
	Nitric oxide (NO) scavenging activity	41.68 ± 2.64	%
	Ferrous ion (Fe^{2+}) chelating activity	14.83 ± 2.40	%

Table 2: Antibacterial activity of *Justicia carnea* and its synthesized nanoparticles

Samples	Antibacterial activity				
	Xanthomonas azonopodis	***Salmonella typhi***	***Pseudomonas aeruginosa***	***Erwinia carotovora***	***Streptococcus mutant***
Extract	1.5	3	13	3	4
ZnNP	8	1	14	6	5
AgNP	4	1	14	8	8
CuNP	7	7	10	3.5	6
Standard (Streptomycin sample)	30	30	35	38	30

AgNPs: silver nanoparticles; ZnNPs: zinc nanoparticles; CuNPs copper nanoparticles; Zone of inhibition in mm.

Table 3: Antifungal activity of *Justicia carnea* and its synthesized nanoparticles

Samples	Antifungal activity		
	Fusarium oxysporium	***PhythophthoraInfestant***	***Aspergillus flavus***
Extract	47.62	28.89	50.78
ZnNP	7.14	2.78	24.94
AgNP	4.76	26.67	25.84
CuNP	21.43	27.78	43.82
Standard (Ketoconazole tablet)	98	98	98

AgNPs: silver nanoparticles; ZnNPs: zinc nanoparticles; CuNPs copper nanoparticles; Percentage growth inhibition (%).

Table 4: Results for molecular docking ΔG (kcal/mol)

Ligand	1EER (Transferrin)	1MIF (MIF)	2HRE(ERα)	3ECU(EPO)	3E7G(DHFR)
β Amyrin	-6.1818	-8.9036	-6.8737	-6.5233	-6.7613
α Amyrin	-6.6296	-7.275	-6.9196	-7.3351	-6.301
Quercetin	-6.8493	-7.468	-6.4937	-6.862	-6.6576
Kaempferol	-6.7855	-6.7529	-6.4437	-6.6885	-6.6303
Rutin	-8.6922	-8.3194	-7.4779	-7.2462	-6.6091
Phytol	-6.9071	-7.0967	-6.952	-7.1954	-6.6091
Rosmarinic acid	-7.1969	-7.1855	-7.2216	-7.0494	-6.7577
Ursolic acid	-7.1006	-8.0617	-6.8869	-7.8239	-6.3091

1EER = Transferrin; 1MIF = Macrophage migration inhibitory factor; 2HRE = Estrogen receptor alpha (ERα); 3ECU = Erythropoietin receptor (EPO); 3E7G = Dihydrofolate reductase (DHFR).

Table 5: Predicted inhibition constants (Ki in µM) derived from ΔG

Ligand	1EER (Transferrin)	1MIF (MIF)	2HRE(ERα)	3ECU(EPO)	3E7G (DHFR)
β Amyrin	29.39	0.3	9.14	16.52	11.05
α Amyrin	13.8	4.64	8.46	4.2	24.04
Quercetin	9.53	3.35	17.36	9.32	13.17
Kaempferol	10.61	11.21	18.89	12.5	13.79
Rutin	0.42	0.8	3.3	4.87	14.29
Phytol	8.64	6.27	8.01	5.31	14.29
Rosmarinic acid	5.3	5.4	5.08	6.8	11.12
Ursolic acid	6.23	1.23	8.94	1.84	23.71

1EER = Transferrin; 1MIF = Macrophage migration inhibitory factor; 2HRE = Estrogen receptor alpha (ERα); 3ECU = Erythropoietin receptor (EPO); 3E7G = Dihydrofolate reductase (DHFR)

Table 6: Best-binding ligand per target with estimated Ki

Target	Best Ligand	Best ΔG (kcal/mol)	Predicted Ki (µM)
1EER (Transferrin)	Rutin	-8.6922	0.42
1MIF (MIF)	β Amyrin	-8.9036	0.3
2HRE (ERα)	Rutin	-7.4779	3.3
3ECU (EPO)	Ursolic acid	-7.8239	1.84
3E7G (DHFR)	β Amyrin	-6.7613	11.05

1EER = Transferrin; 1MIF = Macrophage migration inhibitory factor; 2HRE = Estrogen receptor alpha (ERα); 3ECU = Erythropoietin receptor (EPO); 3E7G = Dihydrofolate reductase (DHFR)

Table 7: ADME properties of phytochemicals

Ligand	GI Absorption	BBB Permeant	CYP Inhibition	Lipinski Violations	Bioavailability Score	Water Solubility
Quercetin	High	No	1/5	1	0.55	Moderately soluble
Kaempferol	High	No	0/5	0	0.55	Soluble
Rutin	Low	No	0/5	2	0.11	Poorly soluble
Ursolic acid	Low	No	3/5	2	0.55	Poorly soluble
Phytol	High	Yes	0/5	1	0.55	Soluble
β Amyrin	Low	No	1/5	2	0.55	Poorly soluble
α Amyrin	Low	No	1/5	2	0.55	Poorly soluble
Rosmarinic acid	High	No	0/5	1	0.55	Soluble

Table 8: Key binding interactions of lead phytochemicals with their protein targets (PLIP analysis)

Ligand – Target	Key Protein Residues	Interaction Types	Notes / Interpretation
β-Amyrin – MIF (1MIF)	Asn98 (H-bond ~2.9 Å); Ile5, Leu59 (Hydrophobic ~3.5–4.2 Å)	1 H-bond, multiple hydrophobics	Stable anchoring of triterpene core; potential to block MIF-driven inflammation (anaemia of chronic disease).
Rutin – Transferrin (1EER)	Asp63, Lys206 (H-bonds 2.7–3.2 Å); Leu/Val (Hydrophobic 3.6–4.2 Å)	Multiple H-bonds, hydrophobics	Dense polar network; strong affinity for iron-binding protein, but poor ADME limits oral bioavailability.
Ursolic acid – MIF (1MIF)	His/Ser (H-bond 2.8–3.1 Å); Phe, Leu, Ile (Hydrophobic cage)	1 H-bond, extensive hydrophobics	Pentacyclic scaffold stabilized in MIF pocket; supports anti-inflammatory potential.
Rosmarinic acid – ERα (2HRE)	Glu353, Asp, His (H-bonds 2.7–3.2 Å)	2–3 H-bonds	Multi-point recognition; likely influences ERα activity and erythropoiesis regulation.

As shown in figure 1, the UV–Visible spectra confirmed nanoparticle formation, with *J. carnea* extract showing a broad band at 300–350 nm and characteristic SPR peaks for AgNPs (≈430 nm), ZnNPs (≈420 nm), and CuNPs (≈450 nm). These peaks reflect successful reduction and stabilization of the metal nanoparticles.

As shown in figure 2, the FTIR spectrum of *J. carnea* aqueous extract exhibited prominent absorption bands at 3371, 2117, 1633, 1017, 637, and 503 cm^{-1}, corresponding to O–H, C≡C, C=O, C–O, and C–H vibrations. These peaks confirm the presence of hydroxyl, carbonyl, and phenolic groups responsible for reducing and stabilizing metal ions during nanoparticle synthesis.

As shown in figure 3, the FTIR spectrum of *J. carnea*-synthesized AgNPs displayed absorption peaks at 3276, 2109, 1633, 1013, 633, and 432 cm^{-1}, corresponding to O–H, C≡C, C=O, C–O, and metal–oxygen vibrations. The similarity of these peaks to those in the extract confirms the involvement of hydroxyl and carbonyl groups in capping and stabilizing the silver nanoparticles.

As shown in figure 4, the FTIR spectrum of *J. carnea*-mediated ZnNPs exhibited major peaks at 3328, 1633, 1017, 622, 521, and 424 cm^{-1}, corresponding to O–H, C=O, C–O, and Zn–O vibrations. These signals confirm the role of phytochemicals—particularly hydroxyl and carbonyl groups—in the reduction and stabilization of zinc nanoparticles.

As shown in figure 5, the FTIR spectrum of *J. carnea*-synthesized CuNPs displayed absorption peaks at 3313, 1633, 626, and 447 cm^{-1}, corresponding to O–H, C=O, and Cu–O vibrations. These peaks confirm the participation of hydroxyl and carbonyl groups from the plant extract in the reduction and stabilization of copper nanoparticles.

The 3D binding interactions of the lead phytochemicals with their respective targets are illustrated in figure 6. These visual representations confirm the predicted hydrogen bonding and hydrophobic interactions observed during molecular docking.

As shown in figure 7, transcription factor enrichment identified STAT5, GATA1/2, HIF1A, RELA (NF-κB), and ESR1 as key regulators linked to erythropoiesis and iron metabolism. The corresponding PPI network revealed strong functional associations among EPO, STAT5, JAK2, HFE, and TFRC, suggesting coordinated modulation of erythropoietic and iron-regulatory pathways.

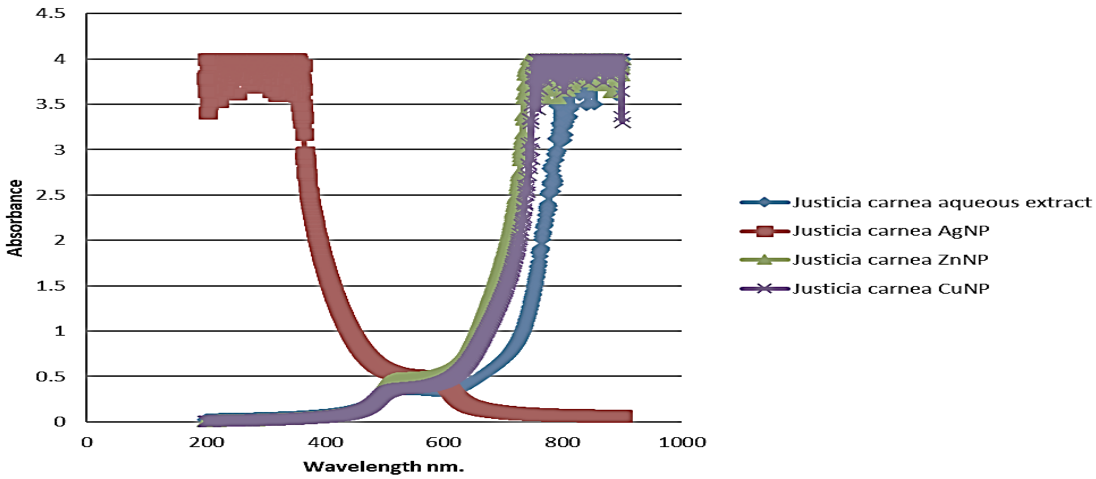

Figure 1: The UV-Visible Characterization of *Justicia carnea* aqeous extract and its synthesized nanoparticles.

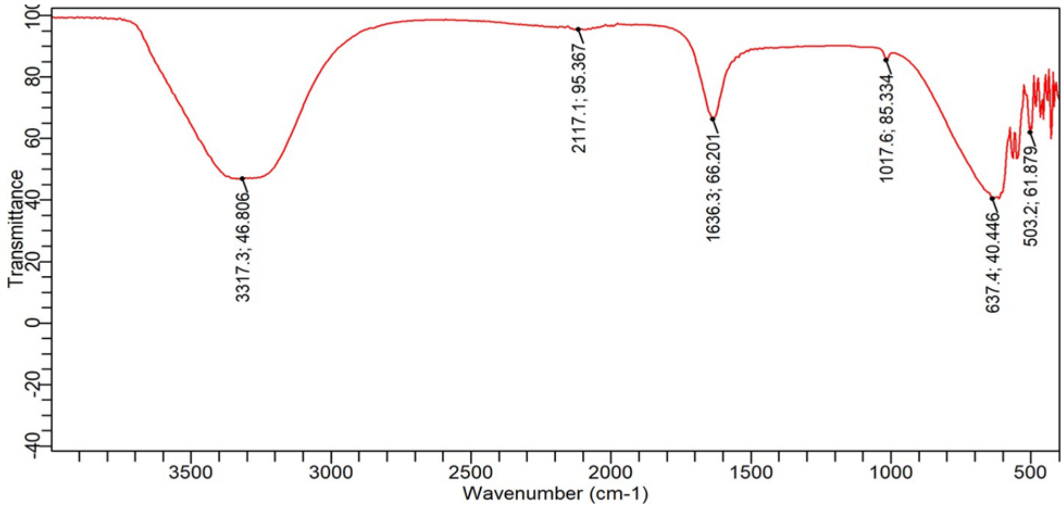

Figure 2: Fourier transform infrared characterization of *Justicia carnea* aqueous extract

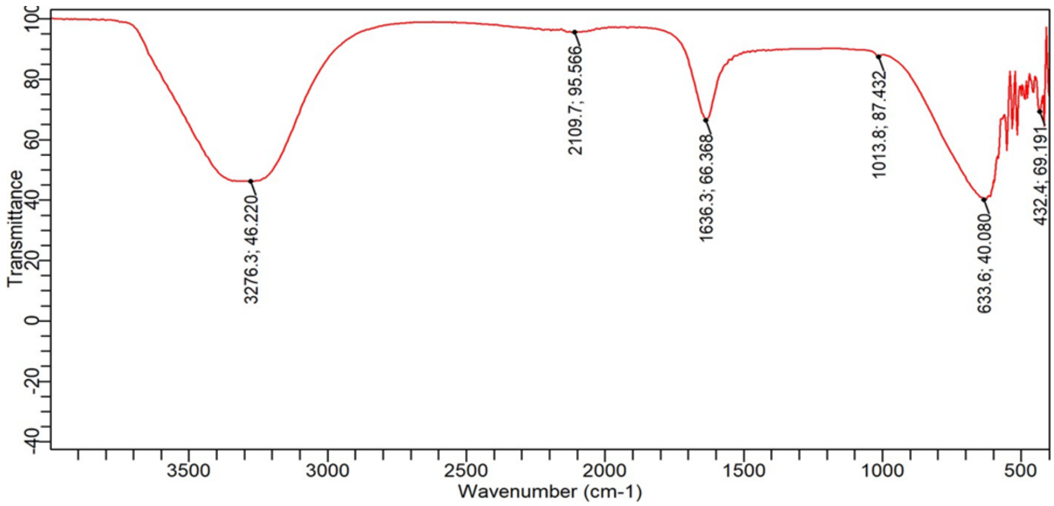

Figure 3: Fourier transform infrared characterization of silver nanoparticles (AgNP)

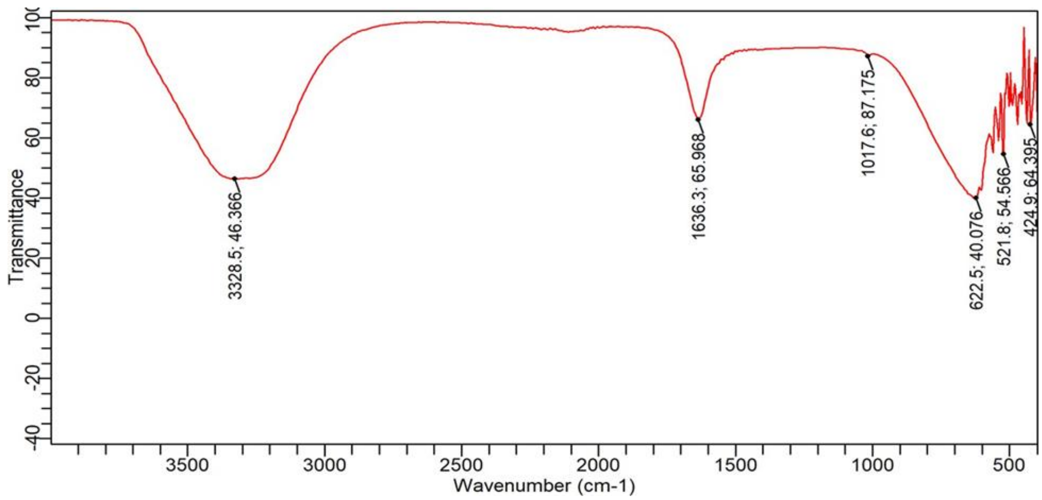

Figure 4: Fourier transform infrared characterization of zinc nanoparticles (ZnNP)

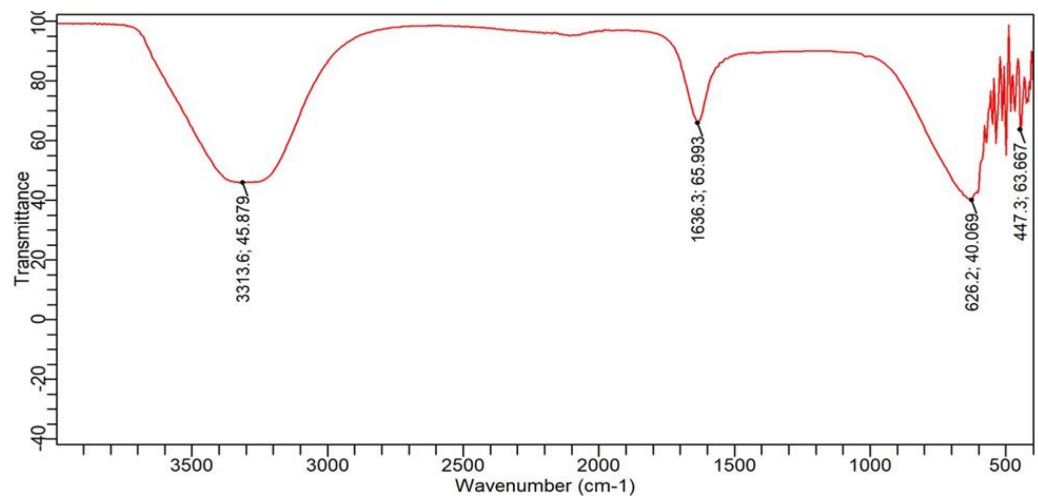

Figure 5: Fourier transform infrared characterization of copper nanoparticles (CuNP)

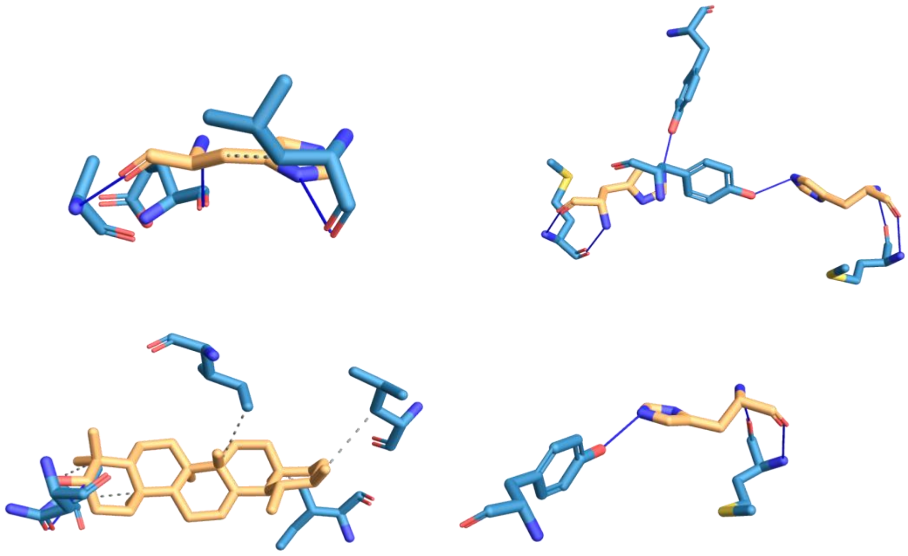

Figure 6: 3D interactions of lead phytochemicals with their protein targets

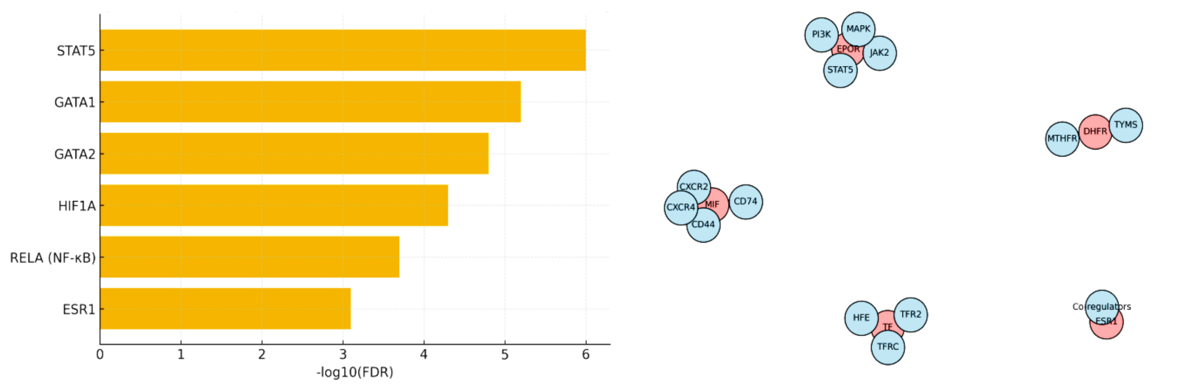

Figure 7: Analysis of transcription factor enrichment (left figure) and protein interaction networks (right figure) of *Justicia carnea* targets

Discussion

This study investigated *J. carnea* and its green-synthesized metallic nanoparticles as potential anti-anaemic agents through combined biochemical evaluation and molecular docking of key phytochemicals. The findings revealed that the plant extract contains diverse bioactive constituents with strong antioxidant and antifungal activities, while the synthesized nanoparticles exhibited enhanced antibacterial effects. Spectroscopic analyses using UV–Vis and FTIR confirmed successful nanoparticle formation and the presence of functional groups associated with capping and stabilization. Molecular docking and ADME analyses indicated that β-amyrin, ursolic acid, rutin, kaempferol, and rosmarinic acid may serve as promising anti-anaemic lead compounds, showing favorable predicted binding to multiple protein targets implicated in red blood cell production.

The presence of multiple secondary metabolites such as saponins, phenols, tannins, terpenoids, alkaloids, and flavonoids. These phytoconstituents are well recognized for their diverse therapeutic relevance, including antimicrobial, antioxidant, anti-inflammatory, and anticancer properties. Comparable metabolite patterns have also been documented in other *Justicia* species and related genera, supporting a shared chemotaxonomic profile (Carneiro et al., 2023; Khedr et al., 2024). The detection of terpenoids and steroidal compounds, in particular, highlights their potential contribution to the plant's bioactivity. Previous findings have linked terpenoid-rich extracts to anti-inflammatory and antimicrobial mechanisms, as well as immunomodulatory effects that enhance host defense responses (Câmara et al., 2024).

The extract displayed pronounced antioxidant activity, particularly through inhibition of lipid peroxidation and nitric oxide radical scavenging. These outcomes can be linked to the abundance of bioactive metabolites such as phenolics, vitamin C, and flavonoids in the plant (Chidi et al., 2020). Phenolic compounds and flavonoids—are known to intercept reactive oxygen species (ROS) and maintain cellular redox balance, thereby minimizing oxidative damage that contributes to degenerative diseases including cardiovascular ailments and various cancers (Huang et al., 2023). Recent investigations have shown that flavonoids exert their cytoprotective and anti-inflammatory effects through modulation of key signalling cascades such as NF-κB and Nrf2 (Zhang et al., 2023). In addition, broad analyses of polyphenol-rich plants have emphasized their multifunctional pharmacological effects, spanning antioxidant, antimicrobial, and disease-preventive mechanisms, which collectively reinforce the medicinal significance of *J. carnea* and related taxa (Liu et al., 2024; Zhao et al., 2025).

The aqueous extract showed moderate antibacterial activity, with inhibition zones ranging from 1.5 to 13 mm, the highest being against *Pseudomonas aeruginosa* (13 mm). In contrast, the nanoparticles—particularly zinc (ZnNPs) and silver (AgNPs) demonstrated enhanced antibacterial effects, recording inhibition zones up to 14 mm, although still below the reference drug streptomycin (30–38 mm). The increased antibacterial efficacy of the nanoparticles is likely due to their nanoscale size, large surface area, and the generation of reactive oxygen species (ROS)that damage microbial membranes, proteins, and DNA, leading to cell death (El Saied et al., 2022).

In antifungal assays, the trend differed. The aqueous extract exhibited the strongest inhibitory effect, achieving 50.78%and 47.62% inhibition against *Aspergillus flavus* and *Fusarium oxysporum*, respectively. The CuNPs showed the highest antifungal activity among the nanoparticles (43.82%), while other nanoparticles displayed lower inhibition levels. The enhanced antifungal activity of the crude extract may be attributed to its rich phenolic and flavonoid compounds, which interfere with fungal cell wall synthesis, ergosterol metabolism, and membrane permeability (AI Aboody & Mickymaray, 2020; Possamai Rossatto et al., 2021). Although all samples exhibited lower activity than the standard antifungal drug ketoconazole (98%), these results collectively indicate that *J. carnea* possesses broad-spectrum antimicrobial potential, with its nanoparticle forms favoring antibacterial effectsand thecrude extract showing stronger antifungal efficacy.

The UV–Vis spectra of *J. carnea* extract and its synthesized nanoparticles, revealing distinct absorption peaks that confirm the successful green synthesis of silver, zinc, and copper nanoparticles. The extract exhibits a broad absorption band between 250 and 400 nm, attributed to phytochemicals such as flavonoids and phenolics. A pronounced surface plasmon resonance (SPR) peak was observed for AgNPs around 400–450 nm, ZnNPs show absorption peaks around 300–350 nm, while CuNPs exhibit a broader peak between 500 and 600 nm. These spectral differences reflect variations in particle size, shape, and stability, with the sharper peaks of AgNPs and ZnNPs suggesting more uniform particles, whereas the broader CuNP peak indicates greater polydispersity (Borah et al., 2022). The higher absorbance observed for AgNPs suggests a higher nanoparticle yield or greater stability (Rivera-Rangel et al., 2021). Each nanoparticle type demonstrates distinct potential applications: AgNPs for antimicrobial use, ZnNPs for UV-blocking and antioxidant functions, and CuNPs for photocatalysis and optoelectronics (Holguín-Meráz et al., 2024; Irede et al., 2024; Tabassum et al., 2025).

The spectra reveal notable shifts and changes in absorption peaks, indicating interactions between metal ions and phytochemicals. Key functional groups, including hydroxyls, aromatics, and alkyne residues play crucial roles in thebioreduction of metal ions and capping of the resulting nanoparticles (Kumar et al., 2025). The appearance of new peaks—especially in ZnNPs and CuNPs—and shifts in existing peaks confirm successful nanoparticle formation and capping by bioactive compounds. These interactions, as evidenced by FTIR analysis, correlate with the enhanced antibacterial activity observed in the synthesized nanoparticles, likely due to improved surface functionalization and bioavailability (Chowdhury et al., 2021).

Docking results showed that several phytochemicals exhibited high predicted binding affinities to anaemia-related proteins. Ursolic acid demonstrated a strong predicted interaction with the erythropoietin (EPO) receptor ($\Delta G = -7.82$ kcal/mol; Ki ≈ 1.84 μM), suggesting a possible role in modulating the EPO–EPOR–JAK2–STAT5 signaling pathway, which governs erythropoiesis (Weiss and Goodnough, 2019). Similarly, rosmarinic acid formed multiple predicted stabilizing hydrogen bonds with estrogen receptor alpha (ERα), aligning with reports that estrogen receptor signaling influences erythropoiesis and iron homeostasis (Michalak et al., 2023).

β-Amyrin and ursolic acid also showed high predicted affinity for macrophage migration inhibitory factor (MIF) ($\Delta G = -8.90$ and -8.06 kcal/mol, respectively). Since MIF-driven inflammation suppresses erythropoiesis, these *in* *silico* results imply a potential anti-inflammatory mechanism that may help restore red blood cell synthesis (Fraenkel et al., 2016). In addition, rutin displayed strong predicted affinity for transferrin (ΔG = −8.69 kcal/mol; Ki ≈ 0.42 μM), which could facilitate iron transport to developing erythrocytes (Shamsi et al., 2023). Even moderate binding of β-amyrin to dihydrofolate reductase (DHFR; ΔG = −6.76 kcal/mol) suggests a possible contribution to folate metabolism, essential for erythroblast maturation. However, these observations are based solely on molecular docking and require in vitro or in vivo validation before any biological conclusions can be drawn.

Despite favorable docking, pharmacokinetic profiling revealed that the strongest binders β-amyrin, ursolic acid, and rutinsuffer from low gastrointestinal absorption and poor solubility, which could limit systemic availability if administered orally. Rutin in particular showed a very low bioavailability score (0.11). In contrast, kaempferol and rosmarinic acid demonstrated high GI absorption, good solubility, and minimal Lipinski violations, indicating better drug-likeness despite their moderate binding energies. This highlights the classic trade-off between binding affinity and drug-likeness: the strongest interactions may identify promising structural leads, whereas compounds with balanced docking and ADME properties are more likely to translate into practical therapeutic candidates. Formulation strategies such as nanoencapsulation, cyclodextrin complexation, or prodrug derivatization could be explored to improve the solubility and absorption of compounds like rutin and ursolic acid, thereby enhancing their pharmacological potential (Gupta et al., 2021; Khan et al., 2022).

Residue-level interaction analysis confirmed that top ligands formed stabilizing contacts within the binding pockets of their respective targets. β-Amyrin established a predicted hydrogen bond with Asn98 of MIF alongside several hydrophobic interactions. Rutin formed hydrogen bonds with Asp63 and Lys206 of transferrin, in addition to hydrophobic anchoring. Ursolic acid interacted with MIF via a carboxylate–His/Ser hydrogen bond and hydrophobic bracing with Phe, Leu, and Ile, while rosmarinic acid established 2–3 hydrogen bonds with Glu353, Asp, and His of ERα. These interactions provide *computational evidence* supporting the potential of these compounds to influence protein stability and function, pending experimental validation.

Network enrichment in revealed that the anaemia-related targets identified through molecular docking—MIF, Transferrin, ESR1, EPOR, and DHFR—are functionally interconnected within pathways governing erythropoiesis, inflammation, and iron metabolism. MIF and EPOR were central nodes in the PPI network, linking inflammatory signaling to erythroid proliferation via the JAK2–STAT5 axis. Transferrin and DHFR clustered within the iron transport and folate biosynthesis modules, respectively, underscoring their complementary roles in haemoglobin synthesis (Zheng et al. 2019). Transcription factor analysis in (Figure 7) further indicated the regulatory influence of GATA1, HIF1A, and NF-κB, which coordinate red blood cell maturation and stress response (Gutiérrez et al., 2020; Bandarra et al., 2014). Collectively, these interactions suggest that *J. carnea* phytochemicals may exert their predicted anti-anaemic effects by modulating multiple transcriptionally regulated pathways involved in erythropoiesis and inflammation.

Conclusion

The findings of this study support the ethnomedicinal relevance of *J. carnea* in the management of anaemia based on molecular docking predictions. The identified phytochemicals demonstrated the ability to interact with multiple biological targets involved in erythropoietin signaling, iron transport, folate metabolism, estrogen regulation, and inflammatory control, which are central to red blood cell production. Docking analysis revealed a two-tier pharmacological potential, with high-affinity triterpenes (β-amyrin, ursolic acid, and rutin) serving as strong mechanistic validators, while more drug-like flavonoids (kaempferol and rosmarinic acid) represent promising candidates for future therapeutic development. In addition, *J. carnea* exhibited notable antioxidant and antimicrobial activities supported by its phenolic and terpenoid composition, with silver and zinc nanoparticles showing enhanced antibacterial activity and the crude extract demonstrating superior antifungal effects. Overall, these results position *J. carnea* as a promising multi-target phytotherapeutic candidate for managing anaemia and related disorders, consistent with earlier reports, while further in vitro and in vivo studies are required to validate these findings.

Declarations

Conflict of Interest

The authors affirm that no potential conflict of interest exist concerning the research, authorship, or publication of this article.

Acknowledgments

The authors wish to state that no formal acknowledgments apply to this work.

Consent for Publications

The authors certify that that this work in its final form has been thoroughly reviewed and approved for publication.

Funding Support

This study was conducted without any form of external funding, sponsorship, or financial assistance.

Authors' Contributions

Conceptualization: Adebayo Seun Gbadamosi, Oloketuyi Kikelomo Boluwatife
Data curation: Adebayo Seun Gbadamosi, Oloketuyi Kikelomo Boluwatife, Margaret Oladunni Oseni, Olatunde Abass Oseni
Formal analysis: Adebayo Seun Gbadamosi, Margaret Oladunni Oseni, Olatunde Abass Oseni
Funding acquisition: Not applicable
Investigation: Adebayo Seun Gbadamosi, Oloketuyi Kikelomo Boluwatife, Margaret Oladunni Oseni, Olatunde Abass Oseni
Methodology: Adebayo Seun Gbadamosi, Oloketuyi Kikelomo Boluwatife, Margaret Oladunni Oseni, Olatunde Abass Oseni
Project administration: Adebayo Seun Gbadamosi, Oloketuyi Kikelomo Boluwatife, Margaret Oladunni Oseni, Olatunde Abass Oseni
Resources: Adebayo Seun Gbadamosi, Oloketuyi Kikelomo Boluwatife, Margaret Oladunni Oseni, Olatunde Abass Oseni
Software: Adebayo Seun Gbadamosi, Oloketuyi Kikelomo Boluwatife, Margaret Oladunni Oseni, Olatunde Abass Oseni
Supervision: Adebayo Seun Gbadamosi, Margaret Oladunni Oseni, Olatunde Abass Oseni
Validation: Adebayo Seun Gbadamosi, Margaret Oladunni Oseni, Olatunde Abass Oseni
Visualization: Adebayo Seun Gbadamosi, Oloketuyi Kikelomo Boluwatife
Writing – original draft: Adebayo Seun Gbadamosi, Oloketuyi Kikelomo Boluwatife
Writing – review & editing: Adebayo Seun Gbadamosi, Oloketuyi Kikelomo Boluwatife, Margaret Oladunni Oseni, Olatunde Abass Oseni

Ethical Considerations

All ethical principles and standards for scholarly research—covering plagiarism, data integrity, originality, and proper citation—were diligently upheld throughout the development and submission of this work.

AI Use Disclosure

The authors confirm that QuillBot AI and Grammarly were used strictly for language editing, grammar correction, and paraphrasing assistance during the preparation of this manuscript. Specifically, these tools were applied to improve clarity, sentence structure, and overall readability in the Abstract, Introduction, Methods, Results, Discussion, and Conclusion sections. No AI tools were used for data generation, experimental design, statistical analysis, molecular docking simulations, or interpretation of results. All AI-assisted content was thoroughly reviewed, edited, and validated by the authors to ensure scientific accuracy, originality, and full compliance with academic and ethical standards.

References

Al Aboody MS, Mickymaray S. Anti-fungal efficacy and mechanisms of flavonoids. *Antibiotics (Basel)*. 2020;9(2):45. doi:10.3390/antibiotics9020045.

Altınsoy Ş, Kızılbey K, İlim HB. Green synthesis of Ag and Cu nanoparticles using *E. telmateia* Ehrh extract: coating, characterization, and bioactivity on PEEK polymer substrates. *Materials*. 2024;17(22):5501. doi:10.3390/ma17225501.

Anarado NI, Eze EA, Agomuo EN. The phytochemistry, ethnomedicinal and pharmacological uses of *Justicia carnea* Lindl used in traditional medicine in Nigeria: a review. South Asian Research Journal of Natural Products. 2021;4(3):234–242.

Atanasov AG, Zotchev SB, Dirsch VM, Supuran CT. Natural products in drug discovery: advances and opportunities. Nature Reviews Drug Discovery. 2021;20(3):200–216. doi:10.1038/s41573-020-00114-z.

Badami S, Aneesh R, Sankar S, Sathishkumar MN, Suresh B, Rajan S. Antifertility activity of Derris brevipes var. coriacea. Journal of Ethnopharmacology. 2003;84(1):99–104. doi:10.1016/S0378-8741(02)00288-X.

Bandarra D, Rocha S, Scholz CC, Wabnitz GH, Schmid T. HIF-1α restricts NF-κB-dependent gene expression to control hypoxic responses. *BMC Research Notes*. 2014;7:292. doi:10.1186/1756-0500-7-292.

Benzie IFF, Strain JJ. The ferric reducing ability of plasma (FRAP) as a measure of antioxidant power: the FRAP assay. Analytical Biochemistry. 1996;239(1):70–76. doi:10.1006/abio.1996.0292.

Berman HM, Westbrook J, Feng Z, Gilliland G, Bhat TN, Weissig H, et al. The Protein Data Bank. Nucleic Acids Research. 2000;28(1):235–242. doi:10.1093/nar/28.1.235.

Borah R, Verbruggen SW. Effect of size distribution, skewness and roughness on the optical properties of colloidal plasmonic nanoparticles. arXiv preprint. 2022. doi:10.48550/arXiv.2202.05729.

Brand-Williams W, Cuvelier ME, Berset C. Use of a free radical method to evaluate antioxidant activity. LWT – Food Science and Technology. 1995;28(1):25–30. doi:10.1016/S0023-6438(95)80008-5.

Câmara JS, et al. Plant-derived terpenoids: a plethora of bioactive compounds with several health functions and industrial applications – a comprehensive overview. Molecules. 2024;29(16):3861. doi:10.3390/molecules29163861.

Carneiro MRB, Sallum LO, Martins JLR, Peixoto JC, Napolitano HB, Rosseto LP. Overview of the Justicia genus: insights into its chemical diversity and biological potential. Molecules. 2023;28(3):1190. doi:10.3390/molecules28031190.

Chidi US, Nnenna AO, Kelechi AK, Chijindu MF, Nebolisa OC. In vitro and in vivo antioxidant activity of ethanol leaf extract of *Justicia carnea*. International Journal of Biochemistry Research and Review. 2020;29(4):48–60. doi:10.9734/ijbcrr/2020/v29i430185.

Chowdhury A, Ara J, Islam MS. Green synthesis of phytochemical nanoparticles and their antimicrobial activity: a review study. Biomedical Journal of Scientific and Technical Research. 2021;34(4):27140–27145. doi:10.26717/BJSTR.2021.34.005580.

Daina A, Michielin O, Zoete V. SwissADME: a free web tool to evaluate pharmacokinetics, drug-likeness and medicinal chemistry friendliness of small molecules. Scientific Reports. 2017;7:42717. doi:10.1038/s41598-017-07854-1.

Dinis TCP, Madeira VMC, Almeida LM. Action of phenolic derivatives as inhibitors of membrane lipid peroxidation and as peroxyl radical scavengers. Archives of Biochemistry and Biophysics. 1994;315(1):161–169. doi:10.1006/abbi.1994.1485.

El Saied FA, Ibrahim AS, El Mokhtar MA. Antibacterial mechanisms of zinc oxide nanoparticles against bacterial food pathogens resistant to beta-lactam antibiotics. Molecules. 2022;27(8):2489. doi:10.3390/molecules27082489.

Fraenkel PG, Badar A, Tipping J. Anemia of inflammation: etiology, pathophysiology, and clinical management. Blood. 2016;127(3):353–361. doi:10.1182/blood-2015-08-618951.

Gfeller D, Grosdidier A, Wirth M, Daina A, Michielin O, Zoete V. SwissDock, a protein–small molecule docking web service based on EADock DSS. Nucleic Acids Research. 2014;42(Web Server issue):W270–W275. doi:10.1093/nar/gku365.

Gowda P, Kumar V, Reddy S, Basavaraja S. Green synthesis and antimicrobial evaluation of metal nanoparticles using plant extracts: a comprehensive study. Journal of Nanobiotechnology. 2023;21(1):118. doi:10.1186/s12951-023-01890-6.

Green LC, Wagner DA, Glogowski J, Skipper PL, Wishnok JS, Tannenbaum SR. Analysis of nitrate, nitrite, and nitrate in biological fluids. Analytical Biochemistry. 1982;126(1):131–138. doi:10.1016/0003-2697(82)90118-X.

Gupta V, Tiwari A, Mishra N. Nanoformulation approaches to improve solubility and bioavailability of phytoconstituents: a review. Journal of Drug Delivery Science and Technology. 2021;66:102829. doi:10.1016/j.jddst.2021.102829.

Gutiérrez L, Caballero N, Fernández-Calleja L, Karkoulia E, Strouboulis J, Suárez-Alvarez B. Regulation of GATA1 levels in erythropoiesis. *International Journal of Molecular Sciences*. 2020;21(3):885. doi:10.3390/ijms21030885.

Harborne JB. Phytochemical methods: a guide to modern techniques of plant analysis. London: Chapman and Hall; 1973.

Holguín-Meráz C, Martínez-Martínez RE, Zaragoza-Contreras EA, Domínguez-Pérez RA, Reyes-López SY, Donohue-Cornejo A, et al. Antibacterial effect of silver nanoparticles against oral biofilms in subjects with motor and intellectual disabilities. Journal of Functional Biomaterials. 2024;15(7):191. doi:10.3390/jfb15070191.

Huang W, Zhong Y, Gao B, Zheng B, Liu Y. Nrf2-mediated therapeutic effects of dietary flavones in different diseases. Frontiers in Pharmacology. 2023;14:1240433. doi:10.3389/fphar.2023.1240433.

Igbinaduwa PO, Kabari KM, Chikwue TC. Phytochemical and anti-anaemic properties of ethanol leaf extract of *Justicia carnea* Vahl. Nigerian Journal of Pharmaceutical and Applied Science Research. 2020;9(2):123–31.

Irede EL, Awoyemi RF, Owolabi B, Aworinde OR, Kajola RO, Hazeez A, et al. Cutting-edge developments in zinc oxide nanoparticles: synthesis and applications for enhanced antimicrobial and UV protection in healthcare solutions. RSC Advances. 2024;14:20992–34. doi:10.1039/D4RA02452D.

Kassebaum NJ, Vos T, Murray CJ. Global burden of anemia: a systematic analysis. The Lancet. 2014;383(9924):1183–94. doi:10.1016/S0140-6736(13)60842-0.

Khan T, Gurav P, Gohil K, Pandey A. Cyclodextrin-based inclusion complexes to enhance solubility and bioavailability of natural products: recent progress and prospects. Phytomedicine. 2022;100:154083. doi:10.1016/j.phymed.2022.154083.

Khedr NM, Ibrahim AA, El-Metwally M, Eldakroory S, Soliman MI. Phytochemical analysis, antioxidant activity, antimicrobial evaluation, and cytotoxicity effects of wild medicinal plants. SABRAO Journal of Breeding and Genetics. 2024;56(4):1552–1562. doi:10.54910/sabrao2024.56.4.21.

Kim S, Chen J, Cheng T, Gindulyte A, He J, He S, et al. PubChem in 2023: new data content and improved web interfaces. Nucleic Acids Research. 2023;51(Database issue):D1373–80. doi:10.1093/nar/gkac1033.

Kumar A, Das S, Singh R. Phytochemical-assisted synthesis, optimization, and characterization of silver nanoparticles. RSC Advances. 2025;15(12):24371–24383. doi:10.1039/D4RA08900F.

Kumar S, Kumbhat R. Carbon nanomaterials: synthesis, properties, and applications. Nanomaterials (Basel). 2016;6(2):43. doi:10.3390/nano6020043.

Liu S, Zhou R, Zhang J, Xu F. Research advances in the bioactivity of plant polyphenols. International Journal of Food Science and Technology. 2024;59(11):8037–8044. doi:10.1111/ijfs.17393.

McLean E, Cogswell M, Egli I, Wojdyla D, de Benoist B. Worldwide prevalence of anaemia, WHO Vitamin and Mineral Nutrition Information System, 1993–2005. Public Health Nutrition. 2011;14(4):430–8. doi:10.1017/S1368980010002669.

Meng XY, Zhang HX, Mezei M, Cui M. Molecular docking: a powerful approach for structure-based drug discovery. Current Computer-Aided Drug Design. 2022;18(4):233–250.

Michalak O, Kostecka A, Cmoch P. Synthesis, biological activity, ADME and molecular docking studies of ursolic acid derivatives. International Journal of Molecular Sciences. 2023;24(10):8875. doi:10.3390/ijms24108875.

Morris GM, Huey R, Lindstrom W, Sanner MF, Belew RK, Goodsell DS, Olson AJ. AutoDock4 and AutoDockTools4. Journal of Computational Chemistry. 2009;30(16):2785–91.

Ohkawa H, Ohishi N, Yagi K. Assay for lipid peroxides in animal tissues by thiobarbituric acid reaction. Analytical biochemistry. 1979;95(2):351-8.

Onyeabo C, Achi NK, Ekeleme-Egedigwe CA, Ebere CU, Okoro CK. Haematological and biochemical studies on *Justicia carnea* leaves extract in phenylhydrazine-induced anaemia in albino rats. Acta Scientiarum Polonorum Technologia Alimentaria. 2017;16(2):217–30. doi:10.17306/J.AFS.0492.

Possamai Rossatto FC, Souza CM, de Bastos JC, Bandeira PT, da Cunha MLR, Pippi B, Oliveira LFS. Antifungal activity of ellagic acid and caffeic acid phenethyl ester against drug-resistant Candida auris. Journal of Fungi. 2021;7(9):763. doi:10.3390/jof7090763.

Rai M, Yadav A, Gade A. Silver nanoparticles as a new generation of antimicrobials. Biotechnology Advances. 2012;30(3):613–22.

Rana A, Yadav KK, Kumar S, Singh J, Gupta N, Yadav S. Recent advances in green synthesis of nanoparticles and their environmental and biomedical applications. Environmental Nanotechnology, Monitoring and Management. 2023;20:100760. doi:10.1016/j.enmm.2023.100760.

Ravera-Rangel RD, Alvarado-Beltrán CG, González-González RB, Zavala-Rivera P, García-Betancourt ML, Gonzalez CM. New hybrid copper nanoparticles/conjugated polyelectrolyte composite with antibacterial activity. Nanomaterials (Basel). 2021;11(2):284. doi:10.3390/nano11020284.

Roe JH, Kuether CA. The determination of ascorbic acid in whole blood and urine. Journal of Biological Chemistry. 1943;147(2):399–407.

Salaudeen IO, Olajuwon MO, Ajala AB, Abdulkareem TO, Adeniyi SA, Jisu SA, et al. Green synthesis, characterization and in vitro antioxidant property of silver nanoparticles using aqueous leaf extract of *Justicia carnea*. Asian Journal of Biochemistry, Genetics and Molecular Biology. 2021;7(3):20–30. doi:10.9734/ajbgmb/2021/v7i330175.

Salem MA, Shaltout KH, Zayed RA, Abd-Elgawad AM. Allium sativum peels extract as a biofungicide. Horticulturae. 2023;9(2):136. doi:10.3390/horticulturae9020136.

Salentin S, Schreiber S, Haupt VJ, Adasme MF, Schroeder M. PLIP: fully automated protein–ligand interaction profiler. Nucleic Acids Research. 2015;43(Web Server issue):W443–W447. doi:10.1093/nar/gkv315.

Schrödinger LLC. The PyMOL molecular graphics system. Version 1.8. New York: Schrödinger; 2015.

Shamsi A, Khan MS, Hassan MI, et al. Molecular interaction of rutin with human transferrin. Journal of Molecular Structure. 2023;1281:135074. doi:10.1016/j.molstruc.2023.135074.

Sharma VK, Yngard RA, Lin Y. Silver nanoparticles: green synthesis and antimicrobial activities. Journal of Nanoparticle Research. 2009;11(7):1823–1831. doi:10.1007/s11051-008-9541-2.

Singh H, Singh M, Pandey A, Sharma R. Revisiting the green synthesis of nanoparticles. International Journal of Nanomedicine. 2023;18:2491–2511. doi:10.2147/IJN.S419369.

Singleton VL, Orthofer R, Lamuela-Raventós RM. Analysis of total phenols. Methods in Enzymology. 1999;299:152–178.

Tabassum S, Sahadat H, Saeed MA, Uddin MN, Ahmed S. Antibacterial and photocatalytic properties of copper oxide nanoparticles. Materials Advances. 2025;6:2338–2355. doi:10.1039/D4MA01047G.

Trease GE, Evans WC. Pharmacognosy. 14th ed. London: W.B. Saunders; 1996.

Weiss G, Goodnough LT. Anemia of inflammation. The Lancet. 2019;393(10191):101–10. doi:10.1016/S0140-6736(18)33265-0.

World Health Organization. The global prevalence of anaemia in women and children: estimates for 2021. Geneva: World Health Organization; 2023. doi:10.4060/cc3093en.

Zhang H, Wang C, Li Y, Chen Y, Liu L. Effects of flavonoids on cancer, cardiovascular and neurodegenerative diseases. International Journal of Molecular Sciences. 2023;24(11):9236. doi:10.3390/ijms24119236.

Zhao J, Yang W, Chen H, et al. Recent advances in tea and other plant polyphenol biomaterials. Beverage Plant Research. 2025;5:e010. doi:10.48130/bpr-0025-0012.

Zhao L, Sun C, Hu Y, Lin C, Wang H. Plant-derived iron supplements: bioavailability, metabolism and therapeutic applications. Food and Function. 2022;13(9):5023–38. doi: 10.1039/D1FO04106K.

Zhishen J, Mengcheng T, Jianming W. Determination of flavonoid contents in mulberry. Food Chemistry. 1999;64(4):555–559. doi:10.1016/S0308-8146(98)00102-2.